

RSC Advances



This is an *Accepted Manuscript*, which has been through the Royal Society of Chemistry peer review process and has been accepted for publication.

Accepted Manuscripts are published online shortly after acceptance, before technical editing, formatting and proof reading. Using this free service, authors can make their results available to the community, in citable form, before we publish the edited article. This *Accepted Manuscript* will be replaced by the edited, formatted and paginated article as soon as this is available.

You can find more information about *Accepted Manuscripts* in the [Information for Authors](#).

Please note that technical editing may introduce minor changes to the text and/or graphics, which may alter content. The journal's standard [Terms & Conditions](#) and the [Ethical guidelines](#) still apply. In no event shall the Royal Society of Chemistry be held responsible for any errors or omissions in this *Accepted Manuscript* or any consequences arising from the use of any information it contains.

**Soft-template mediated approach for Au(0) formation on heterosilica surface
and synergism in catalytic reduction of 4-nitrophenol**

Prateeksha Mahamallik and Anjali Pal*

Department of Civil Engineering, Indian Institute of Technology, Kharagpur 721302, India

RSC Advances Accepted Manuscript

* Author for correspondence: Anjali Pal, Department of Civil Engineering, IIT Kharagpur, India. Phone: 91-3222-281920, FAX: 91-3222-282254, E-mail: anjalipal@civil.iitkgp.ernet.in

Abstract

Under suitably controlled condition cationic surfactant e.g. cetyltrimethylammonium bromide (CTAB) forms bilayers on silica surface, which has the unique property of solubilizing organic molecules through ‘adsolubilization’. This property is judiciously exploited to adsorb AuCl_4^- ion on the modified silica surface at much higher loading (compared to normal silica) through the formation of $\text{CTA}^+ \text{AuCl}_4^-$ complex on silica support. Next, gold nanoparticles supported on surfactant-modified silica (SMS) are prepared using two methods: (1) UV illumination and (2) borohydride reduction, and the materials are designated as SMSG-1 and SMSG-2. Characterization of the particles confirms the formation of Au(0) nanoparticles on SMS surface. Particles have spherical shape with average size 37 ± 11 and 54 ± 14 nm for SMSG-1 and SMSG-2, respectively. They exhibit much higher catalytic activity compared to Au(0) supported on normal silica for 4-nitrophenol (4-NP) to 4-aminophenol (4-AP) reduction in borohydride medium. Such a synergism is presumed to be due to the surfactant bilayer, which provides a high concentration of 4-nitrophenolate ion near Au(0) nanoparticles embodied on SMS leading to highly efficient contact between them. Reductions under different conditions are studied and compared. SMSG-1 shows better performance compared to SMSG-2. While the reaction followed pseudo-first order with SMSG-1 for all experimentally studied conditions, a clear change over in order from first to second was noticed with SMSG-2 under certain conditions. Reaction rates, recycle ability and turn over frequency (TOF) with growing micro-electrode (GME) and full grown micro-electrode (FGME) are compared. GME shows ~9 times higher catalytic activity as compared to FGME.

Keywords: Surfactant-modified silica support; Gold nanoparticle; 4-Nitrophenol; Catalytic reduction; Growing and full grown microelectrode

1. Introduction

The idea of sustainability in research has prompted many scientists to prepare highly potential catalyst material, which can carry out reactions efficiently and selectively. In recent past, metallic nanoparticles have gained tremendous attention because of their potential use in catalysis. Especially nanoparticles on solid support have certain practical benefit. Gold was considered to be chemically inactive till Hutchings's¹ and Haruta's^{2,3} discoveries that gold can be used as catalyst for acetylene hydrochlorination and CO oxidation. One major reason that the gold catalysis did not get attention for many years is that in most cases supported gold nanoparticles prepared by traditional incipient-wetness impregnation method led to nanoparticles with size which was higher than the critical size range thus making them inactive.⁴ To overcome the problem coprecipitation and deposition-precipitation methods were adopted to prepare nanoparticles on oxide support. The catalytic activity of gold depends upon particle size, oxidation state of gold and the nature of supporting materials. The surface of the supporting material acts as nucleating agents and it has the role in stabilizing the nanoparticle which finally may have enormous impacts on the catalytic activity.^{5,6}

Recently heterogeneous gold nanocatalyst materials showed huge demand due to their selective and enhanced catalytic property.⁷ Many researchers have prepared gold nanoparticles on solid support, such as polymer, alumina and silica to enhance the reactivity.⁸ Gold nanoparticle arrays were prepared on poly (N-dodecyl acrylamide-co-4-vinyl pyridine) template.⁹ Scientists have reported gold catalyst preparation on alumina surface by direct anionic exchange (DAE) method.¹⁰ Preparation of gold nanoparticles on anion exchange resin is also reported.^{11,12} Titania doped silica was prepared using sol-gel method and the same material was used for depositing gold on to it.¹³ Gold and silver nanoparticle in either monometallic or

bimetallic forms on calcium alginate beads were prepared using a photochemical method.^{14,15} Spherical polyelectrolyte brushes were used as template for platinum and gold nanoparticle synthesis.¹⁶ Gold nanoparticles were prepared on ZnO-ceramic microstructured paper.¹⁷ Another report discussed about the gold nanoparticle formation on γ -Al₂O₃ support, where plant tannins were the stabilizer.¹⁸ Stabilized gold nanoparticles were also prepared on ~15 nm thin porous alumina sheets.¹⁹ In our work, we have reported the preparation and catalytic application of gold nanoparticles supported on surfactant-modified silica (SMS). Under the specified condition, CTAB molecules get adsorbed on silica surface to form bilayer structure (Scheme 1), which has the capability to 'adsolubilize' various organic molecules at a much higher concentration.²⁰ Preparation of the catalyst material is very simple. Silica, which is used for this material is very cheap. As it is in solid form, the catalyst is very easy to separate from the product.

Nitro aromatic compounds are the most common organic pollutants in industrial and agricultural wastewater. Especially nitrophenols (NPs) are common contaminant in industrial effluent as they are used in manufacturing dyes, explosives and pesticides. 4-Aminophenol (4-AP) is the reduction product of 4-nitrophenol (4-NP). It has immense application as photographic developer, corrosion inhibitor, dyeing agent, building blocks for the production of analgesic and antipyretic drugs. Moreover, in the recent past nanoparticle catalyzed 4-NP reduction by borohydride has received a considerable attention because of its simplicity and reproducibility.^{8,21} The most attractive feature of this benchmark reaction is that it can be monitored using a simple UV-visible spectrophotometer. In our present work, 4-NP reduction has been studied by the prepared materials. It was the focus of the present work to investigate the effect of surfactant bilayer formed on the silica surface, towards the Au(0) formation and 4-NP reduction by borohydride.

2. Materials and Methods

2.1. Chemicals

Sodium borohydride and CTAB were obtained from SRL. Gold chloride (HAuCl_4) was purchased from Aldrich. 4-NP was obtained from LOBA chemicals. It was crystallized from alcohol before use. A stock solution of 4-NP (1×10^{-2} M) was prepared in double distilled water. Silica gel 60-120 mesh size (250 – 150 micron; used for column chromatography) was purchased from Merck. Orange II dye was procured from HIMEDIA.

2.2. Instrumentation

UV-visible spectrophotometer (UV 1, Thermospectronic, England) was used to measure the absorbance with a 1-cm well stoppered quartz cuvette. Fourier transform infrared (FTIR) spectra were obtained using Perkin-Elmer FTIR instrument (RX1). Field Emission Scanning Electron Microscopy (FESEM) was carried out using a microscope (Supra 40, Carl Zeiss Pvt. Ltd, Germany). Transmission electron microscopic (TEM) images were collected by spotting the sonicated sample on a copper grid in a FEI-TECNAI G2 20S-TWIN (USA) instrument with operating voltage 200KV. X-ray diffraction (XRD) analysis of the prepared materials were performed by Bruker axs, SMART APEX II instrument using Cu as the X-ray source with $K\alpha=1.54056$.

2.3. Methods

2.3.1. CTAB determination

The calibration of CTAB was performed following the method reported earlier.²² The procedure involves the ion-association complex formation between Orange II (an anionic dye) and CTAB

(a cationic surfactant) in water medium, and its extraction in chloroform. Finally, the absorbance of the chloroform layer was measured at 485 nm after phase separation. The absorbance value at 485 nm is proportional to the CTAB concentration present in water. The calibration curve is linear in the range of 0-12 mg/L of CTAB. The calibration equation is: Absorbance = $0.066 \times \text{Conc. (mg/L)} + 0.039$ ($R^2 = 0.994$).

2.3.2. Determination of AuCl_4^- loading on silica and surfactant-modified silica (SMS)

HAuCl_4 solution shows an absorption maximum at 222 nm. Concentration of HAuCl_4 adsorbed on SMS and silica was found out from the calibration equation developed for HAuCl_4 at λ_{max} : 222 nm in the concentration range of $0 - 11 \times 10^{-5}$ M. The calibration equation is: Absorbance = $0.1903 \times \text{Conc. (M)} + 0.1105$ ($R^2 = 0.988$). The loading of HAuCl_4 on SMS was calculated to be 6.97×10^{-5} mole of HAuCl_4 per g of SMS. In a similar way loading of HAuCl_4 on normal silica was found to be 3.06×10^{-5} mole of HAuCl_4 per g of silica.

2.4. Preparation of catalyst material

2.4.1. Preparation of surfactant - modified silica (SMS)

Treatment of CTAB with silica under optimized conditions leads to surfactant - modified silica (SMS). The SMS was prepared under predetermined condition following the procedure reported earlier.²³ In a typical procedure silica (30 g), having 60-120 mesh size, was shaken for 2 hours in one liter of CTAB solution having a concentration of 7500 mg/L, which is much higher than the critical micelle concentration (CMC) of CTAB. After shaking for 2 hours, the supernatant was decanted and the silica was washed thoroughly initially with tap water and finally with distilled water. The concentration of CTAB in the supernatant was determined using the procedure described in section 2.3.1 and the loading of CTAB on silica was calculated. The loading of

CTAB on silica surface was found to be 5.7×10^{-4} mole of CTAB / g of silica. The obtained solid material was dried at 60°C for 24 hours, and was designated as surfactant-modified silica (SMS).

2.4.2. Preparation of gold nanoparticle on SMS and silica support

A stock solution of 5×10^{-3} M HAuCl_4 was used for the preparation of the supported gold material. A 25 mL portion of distilled water was added to 12 mL of HAuCl_4 stock solution to make the concentration of HAuCl_4 1.6×10^{-3} M. An aliquot of 37 mL solution was then taken in a 100 mL conical flask and SMS was added to it at a dose of 27.02 g/L. The pH of the medium was about 5. The white color of SMS immediately turned to yellow due to the complexation of surface attached CTA^+ with AuCl_4^- . The material was kept standing for overnight for maximum loading. Same procedure was followed to load AuCl_4^- on silica. Adsorption is ~ 2.3 times more in case of SMS as compared to silica. The supernatant was taken out and the remaining concentration of AuCl_4^- was found out from the pre-established calibration curve. Finally, the loading of AuCl_4^- on SMS was calculated by mass balance method as described in section 2.3.2. The Au(III) loaded SMS material was collected and it was designated as Au(III)-SMS. At the end, Au(III) was reduced to Au(0) following two methods: (1) under UV light illumination, and (2) by sodium borohydride (Scheme 1). In method (1) Au(0) was formed up on ~ 20 min irradiation of UV light ($\lambda \sim 365$ nm; 15 W). The yellow color of the material, which was soaked with little water, turned to dark navy blue. The material was designated as SMSG-1. In method (2), drop wise addition of sodium borohydride (1 M) to Au(III)-SMS resulted in the formation of violet colored Au(0) supported on SMS. The material was designated as SMSG-2. The same two methods described above were also applied for preparing silica-supported Au(0) and the corresponding materials were named as SG-1 (photoreduced) and SG-2 (BH_4^- reduced).

2.5. Experimental for 4-NP reduction

The 4-NP reduction was carried out in a well stoppered quartz cuvette in excess borohydride medium. In a typical set, a mixture of 2.5 mL of BH_4^- and 25 μL of 4-NP (stock solution) was taken in the cuvette and appropriate amount of catalyst was added to it. The reaction was allowed to continue under ambient condition. Stirring was not required because of the liberation of hydrogen gas due to the presence of borohydride. The catalyst was in fluidized condition in the solution due to continuous evolution of bubbles, which favored the reaction. The concentration used for NaBH_4 was 0.1 M in all conditions. The reaction was monitored at 400 nm at different time intervals in a UV-Visible spectrophotometer.

3. Results and Discussions

3.1. Formation of gold nanoparticles on SMS surface

The SMS preparation is interesting and it has enormous applications in pollutant removal through well-known ‘adsolubilization’ mechanism.^{20,23} The point of zero charge (pH_{PZC}) of silica is 1.7.²⁴ Hence at neutral pH its surface is negatively charged. CTAB molecules dissociate into CTA^+ and Br^- in water, and when silica is added to CTAB, CTA^+ ions get attached to the silica surface due to electrostatic interaction forming a monolayer. It is well established that under certain conditions a second layer of surfactant molecules get attached to the first layer through hydrophobic interaction, and finally the positive charge of CTA^+ molecules in the second layer

remains exposed towards the aqueous phase. This type of phenomenon was described earlier through adsorption isotherm studies.^{20,23,25} It is to be noted that the conditions that we applied here for SMS preparation favors the bilayer formation on the silica surface (Scheme 1).²³

After this step, AuCl_4^- ions are adsorbed on the SMS surface (which is a rapid process) and finally reduced to $\text{Au}(0)$. The SMS material shows much higher (~2.3 times) adsorption capacity for AuCl_4^- compared to normal silica, as has been described in section 2.3.2. It reveals that CTAB plays an important role for adsorption of HAuCl_4 on SMS. The loading of AuCl_4^- was indicated by its yellow color which is due to metal-to-ligand charge transfer in AuCl_4^- .¹⁵ The material was very stable (over 6 months) and was designated as Au(III)-SMS. As because gold is the actual catalyst, higher loading of gold in Au(III)-SMS is expected to cause better catalytic efficiency compared to the normal silica material.

The final step of catalyst preparation is the reduction of Au(III) to Au(0) and that has been accomplished by two different methods viz., photochemical and chemical. Although both the routes are available for reduction purposes, photochemical processes are less common. At the same time, while chemical processes suffer from drastic conditions, photochemical processes are more “green” and mild. In the chemical process we have used the most celebrated reagent i.e. sodium borohydride. There are various types of photoinitiators (viz., benzophenone, polyvinylpyrrolidone, polyvinyl alcohol, dendrimers, methanol, benzoin, formic acid, EDTA, Triton X-100, ascorbic acid, alginates etc.) used for reducing gold ion, however in the present case no such initiators are applied for such purpose. The photoirradiation of Au(III)-SMS was done under UV light (~365 nm; 15 W). The material was kept soaked with water during the irradiation time (20 min). The dark navy blue and violet color for the photochemically produced

(SMSG-1) and chemically produced (SMSG-2) materials, respectively were characterized and finally used as the catalysts.

In a similar way AuCl_4^- was also adsorbed on normal silica surface and was finally reduced to Au(0) by the same two methods. It is interesting to observe that the color of these two materials SG-1 and SG-2 prepared by photochemical and chemical method respectively are much less intense. This is due to less gold loading as was described in section 2.3.2.

The whole system acts as a soft template for 4-NP reduction (Scheme 2).

3.2. Characterization of the materials SMSG-1 and SMSG-2

3.2.1. X-Ray diffraction analysis

X-Ray diffraction study (XRD) was carried out for Au(III)-SMS, SMSG-1 and SMSG-2. One broad peak at $2\theta=22^\circ$, which corresponds to amorphous silica is common in all cases (Fig. 1a-c).²⁶ Other peaks for SMSG-1 and SMSG-2 match well with JCPDS file no. 04-0784. The diffraction peaks found at $2\theta = 38.2^\circ, 44.4^\circ, 64.6^\circ, 77.5^\circ, 81.7^\circ$ correspond to {111}, {200}, {220}, {311}, {222} lattice planes, respectively, for face centered cubic lattice structure of gold nanoparticle (Fig. 1b, c). Thus the formation of Au(0) on silica support in both SMSG-1 and SMSG-2 is confirmed.

3.2.2. Scanning electron microscopy

Scanning electron microscopy (SEM) analysis on SMS, Au(III)-SMS, and SMS supported Au(0) (i.e. SMSG-1 and SMSG-2) were performed to have an idea about the particle size and morphology. Figure 2a shows that the SMS surface is smooth. On the other hand the surface of

Au(III)-SMS is rough (Fig. 2b). As observed in Fig. 2c the Au(0) particles prepared photochemically are of spherical shape and they are uniformly distributed on SMS surface. The coverage of Au(0) in SMSG-2 prepared using NaBH_4 , however, is less and the particles are more scattered (Fig. 2d). The size distributions of the particles in SMSG-1 and SMSG-2 are shown in Fig. 2e and f, respectively. The average particle size of Au(0) for SMSG-1 is 37 ± 11 nm and that of SMSG-2 is 54 ± 14 nm.

To know the nature of the surface, SEM analyses were performed on SG-1 and SG-2. The images are shown in Fig. S1 a and b, respectively. Here unlike SMSG-1 and SMSG-2, gold particles are not observed distinctly on the surface, although sufficient loading (3.06×10^{-5} moles per gram of silica) of AuCl_4^- was observed through mass balance method. This is possible because in these cases AuCl_4^- ions have diffused through the silica matrix. In case of SMS, due to the presence of surfactant bilayers on the surface, AuCl_4^- ions attach themselves to the surface. Finally, AuCl_4^- ions are reduced under different conditions.

3.2.3. *Transmission electron microscopy*

Transmission electron microscopy (TEM) analysis provides information about the size and shape of the particles. However, sampling and getting image of SMSG-1 and SMSG-2 was difficult because of the coarse nature of the base material. As an alternative, the materials were dispersed in water by sonication for 15 min. The finer particles those were dispersed in the supernatant were analyzed by TEM. The aggregated nature of the particles is observed from the TEM images of both the materials (Fig. S2 a and b). These particles, as because, come out of the solid support become unstable and in stabilizer-free condition remain aggregated in the aqueous medium. The energy dispersive X-ray spectra (EDAX) confirm the presence of Au in SMSG-1 and SMSG-2.

Figures S2 c and d, and the attached tables indicate that both SMSG-1 and SMSG-2 contain an appreciable amount of gold. The loading of AuCl_4^- in both the cases was the same. However, in SMSG-1 gold is observed in a larger quantity compared to that in SMSG-2, because in SMSG-1 the gold is present more on the surface, whereas in SMSG-2 it diffuses inside the matrix. Such a difference is due to the difference in the preparation procedure of Au(0).

3.2.4. Fourier transform infrared study

To find out the functional groups present in the materials, Fourier transform infrared study (FTIR) was performed and the results are presented in Fig. 3. The broad band at 3484 cm^{-1} has been assigned to O-H stretching of adsorbed water molecules.²⁷ The intense band at 1090 cm^{-1} designates the stretching vibration of Si-O bond.²⁸ Characteristic peak of Si-O-Si was found at 950 cm^{-1} .²⁸ The absorption band at 1227 cm^{-1} and 802 cm^{-1} corresponds to internal and external asymmetric Si-O stretching vibration.²⁹ The absorption at 2939 and 2861 cm^{-1} could be assigned to the asymmetric and symmetric stretching vibration of C-CH₂ group in methylene chain of the adsorbed CTAB.³⁰ Here the peaks are weak because of low loading of CTAB on silica surface.

3.3. Catalytic reduction of 4-nitrophenol

The activity of as-prepared catalysts was demonstrated through 4-NP reduction in presence of borohydride as a reductant. In the last decades this reaction using noble metal nanoparticles as catalyst has become one of the model reactions to evaluate the catalytic activity of various metal nanoparticles viz., Au, Ag, Pd, Pt, Cu etc. present in different substrates. This reaction, although is thermodynamically favorable with $E_0 = -0.76\text{ V}$ for 4-NP/4-AP and -1.33 V vs. NHE for $\text{H}_3\text{BO}_3/\text{BH}_4^-$, but it is kinetically very slow under uncatalyzed condition.

4-NP shows λ_{max} at 317 nm (curve 1, Fig 4a). However, upon addition of NaBH_4 the peak shifts to 400 nm (curve 2, Fig 4a) due to the formation of 4-nitrophenolate anion. An aliquot of 4-NP of concentration $\sim 1.0 \times 10^{-4}$ M was prepared by diluting the stock (10^{-2} M) in borohydride medium (0.1 M), and it was allowed to remain as such for 24 h and the peak at 400 nm was monitored time to time. In this case neither a decrease in absorbance at 400 nm nor a new peak is observed. In presence of SMS and borohydride, however, a slight decrease in absorbance was noticed after 20 min (curve 3, Fig. 4a). This slight decrease in the absorption peak is due to the adsorption of nitrophenolate ion on SMS. But still no new peak related to its reduced product 4-AP was observed at ~ 293 nm (Fig. 4a).

On the contrary, the catalytic activity of SMSG-1 is demonstrated convincingly in Fig. 4b by the spectrophotometric studies. Curve 1 in Fig. 4b depicts the absorption spectrum of 4-NP in absence of borohydride. The shift of the peak at 400 nm in presence of excess borohydride is due to the 4-nitrophenolate anion. After the addition of catalyst SMSG-1, immediately the absorbance at 400 nm went on decreasing with time and a new peak of 4-AP as a product was observed to appear at 293 nm. The sequential decrease in intensity of 400-nm peak is shown in Fig. 4b). This could also be visualized by eyes as the yellow color of the nitrophenolate ion faded and disappeared quickly. In the present study some isobestic points are clearly observed which implies that 4-AP is the sole product during the reaction.³¹ Some isobestic points are not so prominent because of the hindrance in monitoring due to the liberation of gas bubbles.³²

It is interesting to note that the reduction of 4-NP under similar conditions is very fast in presence of Au(III)-SMS (curve 4, Fig. 4a). The reason behind this is discussed more elaborately in section 3.3.2.

The same reaction of 4-NP reduction was carried out with other three prepared catalysts i. e. SG-1, SG-2, and SMSG-2. Rate of the reactions with SG-1 and SG-2 are very slow as compared to SMSG-1 and SMSG-2 for same initial concentration (1.0×10^{-4} M) of 4-NP and catalyst dose (4.0 g/L). Pseudo-first order reaction rate constant of the reaction is 0.001 min^{-1} for SG-1 and SG-2, whereas those with SMSG-1 and SMSG-2 are 0.127 and 0.073 min^{-1} , respectively (Fig. 5).

It is well accepted that the actual catalyst is the gold nanoparticle embedded in the SMS surface. It is already mentioned that gold loading is ~ 2.3 times higher in SMSG compared to that of SG. Hence one factor for enhanced catalysis in SMSG might be the enhanced loading of gold in SMS as compared to silica. However, to account for an enormously enhanced rate (~ 127 times for SMSG-1 and ~ 73 times for SMSG-2 as compared to SG) of 4-NP reduction, there must be some other factors operating. Such an enormous increase in rate is possibly due to facilitated adsorption (or more appropriately adsolubilization) of 4-NP on surfactant bilayer formed on SMSG surface. The high activity arises from the synergistic effect of CTA⁺ bilayer, which provides a high concentration of 4-nitrophenolate ion near to the Au nanoparticles embedded on SMS leading to highly efficient contact between them.

To investigate the effects of adsorbed surfactant bilayer and the embedded gold, detailed kinetic studies were conducted with SMSG-1 and SMSG-2.

3.3.1. Kinetic study

The catalytic reduction of 4-NP in presence of NaBH_4 was reported to follow pseudo-first order reaction in most cases.^{17,33,34} As the concentration of NaBH_4 is very high compared to that of 4-

NP, the reaction has been considered to be almost independent of NaBH_4 concentration (i.e. zero order w.r.t. BH_4^-). In the present case, for SMSG-1 catalyzed reaction, for all experimental catalyst doses (1.78 – 5.0 g/L), the plot of A_0/A vs. time and $\ln A_0/A$ vs. time at 300K are shown in Fig 6a and b, respectively. It is clear from the linear plots of $\ln A_0/A$ vs. time that the reaction follows pseudo-first order kinetics in all cases. The plot of first order rate constants vs. catalyst doses shows good linear correlation (Fig. 6c; $R^2 = 0.994$). The rate of reaction becomes faster with increase in dose (Table 1). It indicates that the reaction is pseudo-first order in the entire range of doses applied. Interestingly, a change in order of kinetics from first order to second order was observed for SMSG-2 while the dose of catalyst is decreased from 5.0 to 1.78 g/L. Keeping the 4-NP concentration fixed at 1.0×10^{-4} M, for dose 1.78, 3.0, and 3.5 g/L the kinetics follows second order, whereas, for dose 4.0 and 5.0 g/L it is noticed to be first order (Fig. S3 and Table 1). Similar phenomenon has been observed with a fixed catalyst dose but varying initial concentrations of 4-NP. For example, at a fixed catalyst dose of 4.0 g/L, the reduction with 0.4×10^{-4} M and 0.6×10^{-4} M 4-NP follows second order but that with 1.0×10^{-4} M and 1.2×10^{-4} M concentration the reaction follows first order (Fig. S3 and Table 1). On the other hand, unlike SMSG-2, in case of SMSG-1 the rate follows first order even with variation of initial 4-NP concentration in the range 0.4×10^{-4} – 1.2×10^{-4} M keeping the catalyst dose fixed at 4.0 g/L. The rate constant is found to decrease drastically from 0.253 to 0.086 min^{-1} as the 4-NP concentration is increased from 0.4×10^{-4} M to 1.2×10^{-4} M (Table 1). Plot of rate constant vs. concentration of 4-NP follows a straight line curve with $R^2=0.969$ (Fig. 7). The comparative account of the first- and second-order rate constants and their correlation coefficient values for all the concentrations of 4-NP and all doses of SMSG-1 and SMSG-2 are compiled in Table 1. From the results it is obvious that SMSG-1 is a better catalyst compared to SMSG-2 for 4-NP

reduction. Rate constant of the reactions could be explained well by Langmuir-Hinshelwood kinetics.^{35,36} The assumption of this mechanism is that the reactants should get adsorbed on the surface of the catalyst. The reaction of the adsorbed species determines the rate. In many cases an induction time was observed for metal nanoparticle induced 4-NP reduction. It designates the surface restructuring of the nanoparticle before starting the reaction.³¹ If rate of reaction between dissolved oxygen present in water and borohydride is faster than that with nitrophenol, then also induction time may be observed.¹⁴ In the present study, however, no induction time is noticed. It is similar with the results presented earlier.¹⁴ As soon as the catalyst is added to the reactant, the reaction starts. Borohydride ion transfers hydride species on the surface of the nanoparticle. This reaction is reversible. Nitrophenol molecules are adsorbed on the surface of the nanoparticle and are reduced by surface hydride species.¹⁶ This adsorption step is also reversible. However, adsorption-desorption equilibrium is reached very fast. The positive charge on the SMSG surface creates favorable condition for the adsorption of both hydride ion and nitrophenolate ion on the surface. This makes the reaction faster. This is clear from the synergism that we observe when SMSG is used as catalyst. After the reaction, the product molecules get desorbed from the surface making the reaction site free for further reaction. Overall conversion of 4-NP to 4-AP is a 6 electron transfer process. According to Gu et al.³¹ the production of 4-AP from 4-NP completes in two steps. In the first step an intermediate, 4-hydroxylaminophenol (4-HAP), a stable product, is formed from 4-NP. Then it gets reduced to the final product, 4-AP. First step is much faster as compared to the second one. The availability of active surface on the nanoparticle decreases as the reaction proceeds, because, during the reduction of 4-NP, concentration of 4-HAP increases with time and it contests with 4-NP for nanoparticle surface.

Kuroda et al.³⁴ have used PMMA as support for gold nanoparticle and the reported nitrophenol reduction rate constant was $7.2-7.9 \times 10^{-3} \text{ sec}^{-1}$. Gao et al.³⁷ and Fenger et al.³⁸ have used almost same quantity of gold but the rate is slightly more in case of Gao et al. In another report by Koga and Kitaoga¹⁷ Au-ZnO is applied to 4-NP reduction while the dose of catalyst is 0.985 g/L. But still its rate of the reaction is comparable to that reported in Au/CTAB study.³⁸ In our work, in case of SMSG-1, the rate can be compared with Au/graphene work.³⁹ Some selected reports are considered for comparing the pseudo-first order rate constants and the operational conditions for 4-NP reduction (Table 2).

3.3.2. Kinetics of 4-NP reduction in growing micro-electrode (GME) and full grown micro-electrode (FGME)

It is well known that the reduction potential of gold is dependent on its size.^{41,42} The progressive decrease in size of metal nanoparticles is accompanied by a stepwise decrease in redox potential value. Thus small metal nanoparticles attain a very low redox potential for a metal(aq)ⁿ⁺ / metal(atom) system. This can enhance the catalytic activity. Keeping this idea in mind, the 4-NP reduction was studied with growing metal nanoparticles⁴³ called 'growing micro-electrode (GME)' and full grown metal nanoparticles called 'full grown micro-electrode (FGME)' on SMS surface. For this experiment 0.01 g Au(III)-SMSG (i.e. at a dose of 0.2 g/L) was added to a mixture of 4-NP (50 mL; $1.0 \times 10^{-4} \text{ M}$) and NaBH₄ (0.1 M), and the kinetics of 4-NP reduction was monitored. The yellow color of the powder turned to violet immediately because of the formation of Au(0), as it was added to 4-NP/BH₄⁻ mixture. During its initial stage, the material can be considered as SMS supported GME and designated as SMS-GME. In this case, the 4-NP

reduction followed second order (as observed from the linear plot of $1/\text{Absorbance}$ vs. time) and the rate constant of the reaction was $0.0766 \text{ mg}^{-1} \text{ lit min}^{-1}$ (Fig. 8a and Table 1). To compare the results with FGME, 0.01 g of SMSG-2 was added to an identical mixture of 4-NP (50 mL; $1.0 \times 10^{-4} \text{ M}$) and NaBH_4 (0.1 M). It was observed that the reaction with SMSG-2 took much longer time; however, it followed second order kinetics (Fig. 8b). The rate constant of the reaction with FGME was $0.002 \text{ mg}^{-1} \text{ lit min}^{-1}$ (Table 1). In case of GME the particles are in the formation stage, whereas, in FGME the nanoparticles are preformed. Thus GME is catalytically more active than FGME due to smaller size of the nanoparticles.

3.3.3. *Recycle ability of the catalysts*

The recycle ability of the catalyst is an important factor. In our study the recycle ability of SMSG-1 and SMS-GME for 4-NP reduction was evaluated. In case of SMSG-1, after ~81% completion of first cycle in 70 min (Fig. 9a), the reaction mixture was allowed to settle, the supernatant was removed carefully and then a fresh lot of 4-NP was added to the already used catalyst. The initial concentration of 4-NP in both the cycles was $1.0 \times 10^{-4} \text{ M}$, and the catalyst dose applied was 1.78 g/L. The efficiency for the second cycle after 70 min of reaction was noted to be ~ 64% with a decrease in reaction rate constant from 0.0248 min^{-1} to 0.0144 min^{-1} (Fig. 9a). The reduced activity is either due to the surface inactivation of the catalyst during the reaction or due to the adsorption of the product molecules.

To examine the recycle ability of SMS-GME, the Au(III)-SMS was added (at a dose of 0.5 g/L) to a mixture of 4-NP ($1.0 \times 10^{-4} \text{ M}$) and NaBH_4 (0.1 M). The color of the material changed immediately from yellow to violet. Au (III) got reduced to Au (0) by NaBH_4 *in situ*, and

simultaneously 4-NP was reduced to 4-AP in the presence of embryonic Au (0). In this case, the particle size is very small as it is in the formation stage. These small embryonic particles are called as growing micro-electrode (GME), and they have very high catalytic activity. In the first cycle with SMS-GME the reduction is found to be ~57 % in 10 min reaction time and the rate constant is found as $0.153 \text{ mg}^{-1} \text{ lit min}^{-1}$. In the second cycle the percent reduction is decreased to ~41% (in 60 min reaction time duration) with rate constant $0.017 \text{ mg}^{-1} \text{ lit min}^{-1}$. Thus the rate is ~9 times lower compared to that observed in the first cycle (Fig. 9b). In the second cycle SMS-GME comprises of already formed gold nanoparticle, and the material is no longer considered as the GME but it is FGME.

To examine whether CTAB is leached from the SMSG surface, the CTAB concentration in the reaction mixture was determined after borohydride reduction of 4-NP and no leaching of CTAB was noticed to take place. Also no Au(0) surface plasmon was observed after the reaction indicating that Au(0) was not leached during the 4-NP reduction. This says that the catalyst is stable. To understand whether there is any change in the crystalline nature of Au(0) after 4-NP reduction, XRD analysis of the used catalyst after the first cycle was performed. The results shown in Fig. S4 reveal that the gold catalyst still retains its crystalline character.

3.3.4. Turn over number (TON) and turn over frequency (TOF) of the catalysts

The TON and TOF values speak about the efficiency of the catalyst. In our studies with both SMSG-1 and SMSG-2, using $1.0 \times 10^{-4} \text{ M}$ 4-NP concentration and 4.0 g/L catalyst dose, the TON is found to be 1.505×10^{22} molecule/g, and the TOF values are found to be 1.19×10^{19} and

0.83×10^{19} molecule/g/s for SMSG-1 and SMSG-2, respectively, which is much higher compared to that with Au(0) on calcium alginate beads.¹⁴

It is encouraging to observe that for SMS-GME the TON and TOF values are 1.2×10^{23} molecule/g and 20.07×10^{19} molecule/g/s, which are much higher compared to those of SMSG-1 or SMSG-2. In this study the initial 4-NP concentration applied is 1.0×10^{-4} M and the catalyst dose is 0.5 g/L. The higher efficiency of the GME is due to the smaller particle size (which relates to larger surface area) and freshly evolved surface of the gold catalyst.

4. Conclusions

Silica upon treatment with CTAB under specified condition forms adsorbed surfactant bilayer which has unique capability of adsolubilizing organic molecules. The effect of this micellar environment for Au(0) formation and its catalytic application on 4-NP reduction has been investigated for the first time. Gold nanoparticle supported on surfactant-modified silica was prepared by two different methods: (1) photoactivation; (2) borohydride reduction. The XRD studies of the materials confirm the formation of Au(0) on the surface. SEM images reveal the distributions of gold nanoparticle on SMS surface. FTIR analysis gives information about the peaks of the supporting material, i.e silica and CTAB. Both the nanoparticles are applied as catalyst for 4-NP reduction in NaBH_4 medium in ambient condition. The kinetics and the mechanism are discussed. The surfactant bilayer present in the silica surface has a great synergistic effect on both gold loading and on the catalytic activity for 4-NP reduction. The catalytic activity of GME and FGME are compared. The rate of reduction with SMS-GME was noted to be ~9 times faster than FGME, while 0.5 g/L of dose and 1.0×10^{-4} M of 4-NP are used.

Acknowledgement

The authors are thankful to IIT Kharagpur for providing the instrumental facility and financial support.

References

- 1 G. Hutchings, *J. Catal.*, 1985, **96**, 292-295
- 2 M. Haruta, T. Kobayashi, H. Sano and N. Yamada, *Chem. Lett.*, 1987, **16**, 405-408.
- 3 M. Haruta, N. Yamada, T. Kobayashi and S. Iijima, *J. Catal.*, 1989, **115**, 301-309.
- 4 Y. Chen, J. Qiu, X. Wang and J. Xiu, *J. Catal.*, 2006, **242**, 227-230.
- 5 A. Wolf and F. Schuth, *Appl. Catal. A: General*, 2002, **226**, 1-13.
- 6 M. M. Schubert, S. Hackenberg, A. C. Veen, M. Muhler, V. Plzak and R. J. Behm, *J. Catal.*, 2001, **197**, 113-122.
- 7 T. Mitsudome and K. Kaneda, *Green Chem.*, 2013, **15**, 2636-2654.
- 8 J. Noh and R. Meijboom, 'Reduction of 4-nitrophenol as a model reduction for nanocatalysis' in "Application of Nanotechnology in Water Research" A. K. Mishra (ed.), Chapter 13, pp. 333-406, Scrivener Publishing LLC (2014).
- 9 H. Tanaka, M. Mitsuishi, T. Miyashita, *Langmuir*, 2003, **19**, 3103-3105.
- 10 S. Ivanova, C. Petit and V. Pitchon, *Appl. Catal. A: General*, 2004, **267**, 191-201.
- 11 S. Praharaj, S. Nath, S. K. Ghosh, S. Kundu, T. Pal, *Langmuir*, 2004, **20**, 9889-9892.
- 12 S. Panigrahi, S. Basu, S. Praharaj, S. Pande, S. Jana, A. Pal, S. K. Ghosh, T. Pal, *J. Phys. Chem. C*, 2007, **111**, 4596-4605.
- 13 L. X. Xu, C. H. He, M. Q. Zhu, K. J. Wu and Y. L. Lai, *Catal. Lett.*, 2007, **118**, 248-253.
- 14 S. Saha, A. Pal, S. Kundu, S. Basu and T. Pal, *Langmuir*, 2010, **26**, 2885-2893.
- 15 S. Saha, A. Pal, S. Pande, S. Sarkar, S. Panigrahi, T. Pal, *J. Phys. Chem. C*, 2009, **113**, 7553-7560.

- 16 S. Wunder, F. Polzer, Y. Lu, Y. Mei and M. Ballauff, *J. Phys. Chem. C*, 2010, **114**, 8814-8820.
- 17 H. Koga and T. Kitaoka, *Chem. Eng. J.*, 2011, **168**, 420-425.
- 18 X. Huang, X. Liao and B. Shi, *Green Chem.*, 2011, **13**, 2801-2805.
- 19 J. Wang, A. H. Lu, M. Li, W. Zhang, Y. S. Chen, D. X. Tian and W. C. Li, *ACS Nano*, 2013, **7**, 4902-4910.
- 20 S. Koner, A. Pal and A. Adak, *Desalination*, 2011, **276**, 142-147.
- 21 T. Aditya, A. Pal and T. Pal, *Chem. Comm.*, 2015, **51**, 9410-9431.
- 22 A. V. Few and R. Ottewill, *J. Coll. Sci.*, 1956, **11**, 34-38.
- 23 S. Koner, A. Pal and A. Adak, *Desalin. Water Treat.*, 2010, **22**, 1-8.
- 24 S. Musić, N. Filipović-Vinceković and L. Sekovanić, *Brazilian J. of Chem. Engg.*, 2011, **28**, 89-94.
- 25 K. Esumi, "Adsolubilization of organic pollutant", In Encyclopedia of Surface and Colloid Science, P. Somasundaran (ed.), 2nd Edition, Vol. 1, CRC Press (2006).
- 26 G. Nallathambi, T. Ramachandran, V. Rajendran and R. Palanivelu, *Mater. Res.*, 2011, **14**, 552-559.
- 27 S. Reddy, B. E. K. Swami and H. Jayadevappa, *Electrochimica Acta*, 2012, **61**, 78-86
- 28 X. K. Ma, N. H. Lee, H. J. Oh, J. W. Kim, C. K. Rhee, K. S. Park and S. J. Kim, *Coll. Surf. A: Physicochem. Eng. Asp*, 2010, **358**, 172-176.
- 29 C. Huo, J. Ouyang and H. Yang, *Scientific Reports*, 2014, **4**.

- 30 O. Yayapao, T. Thongtem, A. Phuruangrat, and S. Thongtem, *J. Alloys and Compounds*, 2011, **509**, 2294-2299.
- 31 S. Gu, S. Wunder, Y. Lu, M. Ballauff, R. Fenger, K. Rademann, B. Jaquet and A. Zaccone, *J. Phys. Chem. C*, 2014, **118**, 18618-18625.
- 32 M. Li and G. Chen, *Nanoscale*, 2013, **5**, 11919-11927.
- 33 M. L. Wang, T. T. Jiang, Y. Lu, H. J. Liu and Y. Chen, *J. Mater. Chem. A*, 2013, **1**, 5923-5933.
- 34 K. Kuroda, T. Ishida and M. Haruta, *J. Mol. Catal. A: Chem.*, 2009, **298**, 7-11.
- 35 N. C. Antonels and R. Meijboom, *Langmuir*, 2013, **29**, 13433-13442.
- 36 S. Gu, J. Kaiser, G. Marzun, A. Ott, Y. Lu, M. Ballauff, A. Zaccone, S. Barcikowski, P. Wagener, *Catal. Lett.*, 2015, **145**, 1105–1112
- 37 Y. Gao, X. Ding, Z. Zheng, X. Cheng and Y. Peng, *Chem. Comm.*, 2007, **36**, 3720-3722.
- 38 R. Fenger, E. Fertitta, H. Kirmse, A. F. Thünemann and K. Rademann, *Phys. Chem. Chem. Phys.*, 2012, **14**, 9343-9349.
- 39 J. Li, C. Y. Liu and Y. Liu, *J. Mater. Chem.*, 2012, **22**, 8426-8430.
40. S. Wang, J. Zhang, P. Yuan, Q. Sun, Y. Jia, W. Yan, Z. Chen, Q. Xu, *J. Mater. Sci.*, 2015, **50**, 1323-1332.
- 41 J. Belloni, *Curr. Opin. Coll. Interf. Sci.* 1996, **1**, 184-196.
- 42 A. Henglein, *J. Phys. Chem.*, 1993, **97**, 5457-5471.
- 43 N. Pradhan, A. Pal and T. Pal, *Coll. Surf. A: Physicochem. Eng. Asp.*, 2002, **196**, 247-257.

Figure & Scheme Caption

Scheme 1: Schematic of SMS and SMSG preparation

Scheme 2: Schematic of 4-NP reduction on SMSG surface

Fig. 1: XRD spectra of (a) SMS and Au (III)-SMS, (b) SMSG-1 (c) SMSG-2

Fig. 2: SEM images of (a) SMS, (b) Au (III)-SMS, (c) SMSG-1, (d) SMSG-2. (e) and (f) shows the size distribution of Au(0) particles in SMSG-1 and SMSG-2, respectively.

Fig. 3: FTIR spectra of (1) SMS, (2) Au(III)-SMS, (3) SMSG-1, (4) SMSG-2

Fig. 4: (a) Absorption spectra of 4-NP under different conditions. Curve 1: 4-NP, curve 2: 4-NP+NaBH₄ (immediate), curve 3: 4-NP+SMS+NaBH₄ (after 20 min), curve 4: 4-NP+Au(III)-SMS+NaBH₄ (after 20 min) (Initial concentration of 4-NP = 1.0×10^{-4} M; Catalyst dose = 4 g/L).

(b) Time dependent absorption spectra for the catalytic reduction of 4-NP in NaBH₄ medium by SMSG-1 as catalyst. Curve 1: 4-NP. (Initial concentration of 4-NP = 1.0×10^{-4} M; Catalyst dose = 3 g/L)

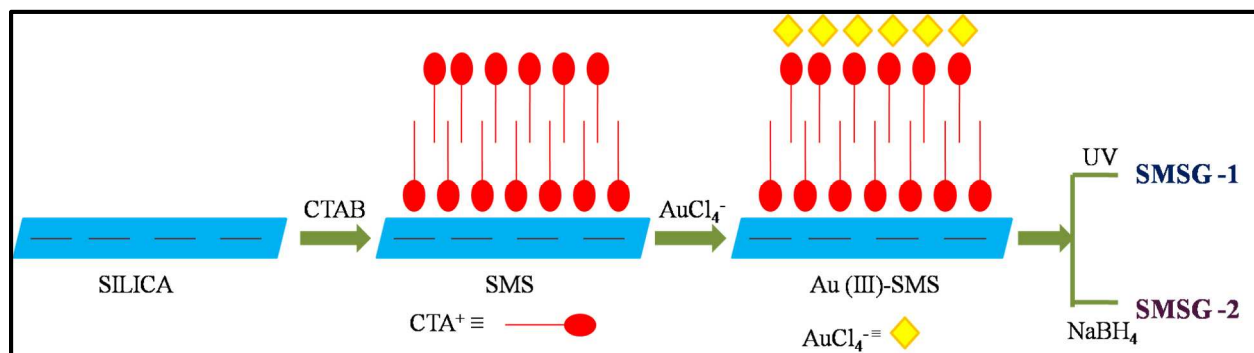
Fig. 5: A comparative account of pseudo-first order rate constant for 4-NP reduction using prepared catalysts SG-1, SMSG-1, SG-2 and SMSG-2 (Initial concentration of 4-NP = 1.0×10^{-4} M; Catalyst dose = 4 g/L)

Fig. 6: Kinetics of 4-NP reduction in presence of SMSG-1 at different doses. (a) Plot of A_0/A vs. time. (b) Plot of $\ln A_0/A$ vs. time, (c) Plot of rate constant vs. catalyst dose (Initial concentration of 4-NP = 1.0×10^{-4} M, Concentration of NaBH₄ = 0.1 M)

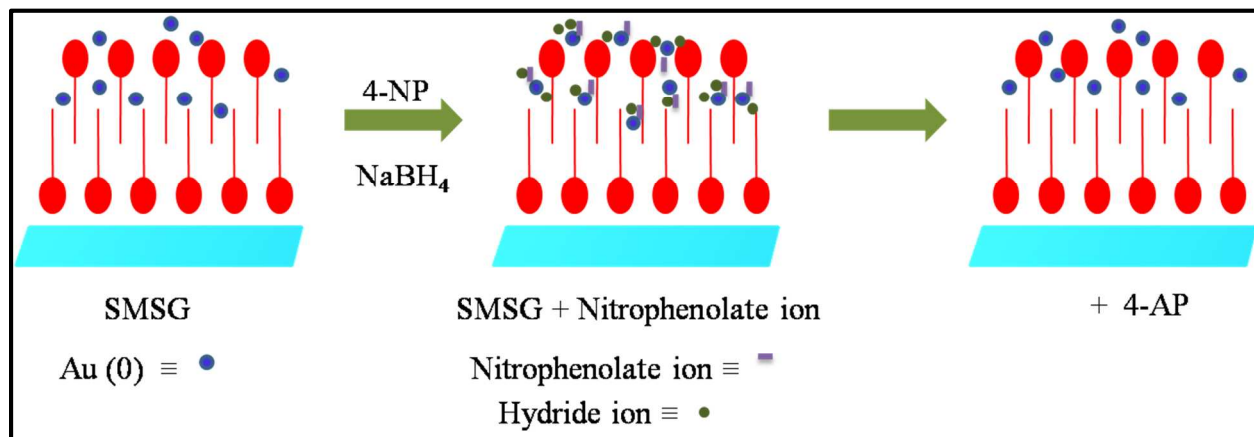
Fig. 7: Plot of rate constant vs. initial concentration of 4-NP for SMSG-1 (Catalyst dose = 4.0 g/L, Concentration of NaBH₄ = 0.1 M)

Fig. 8: (a) 1/Absorbance vs. time plot for 4-NP reduction with SMS-GME as catalyst, (b) 1/Absorbance vs. time plot with SMSG-2 (Initial concentration of 4-NP = 1.0×10^{-4} M, Dose of the catalyst = 0.2 g/L, Concentration of NaBH_4 = 0.1 M)

Fig. 9: (a) Plot of efficiency (after 70 min of reaction for both the cycles) and rate constant of 4-NP reduction in 1st and 2nd cycle using SMSG-1 (Initial concentration of 4-NP = 1.0×10^{-4} M, Catalyst dose = 1.78 g/L, Concentration of NaBH_4 = 0.1 M). (b) Plot of efficiency (after 10 min in case of 1st cycle and after 60 min in case of 2nd cycle) and rate constant of 4-NP reduction in 1st and 2nd cycle for SMS-GME (Initial concentration of 4-NP = 1.0×10^{-4} M, Catalyst dose = 0.5 g/L, Concentration of NaBH_4 = 0.1 M)



Scheme 1: Schematic of SMS and SMSG preparation



Scheme 2: Schematic of 4-NP reduction on SMSG surface

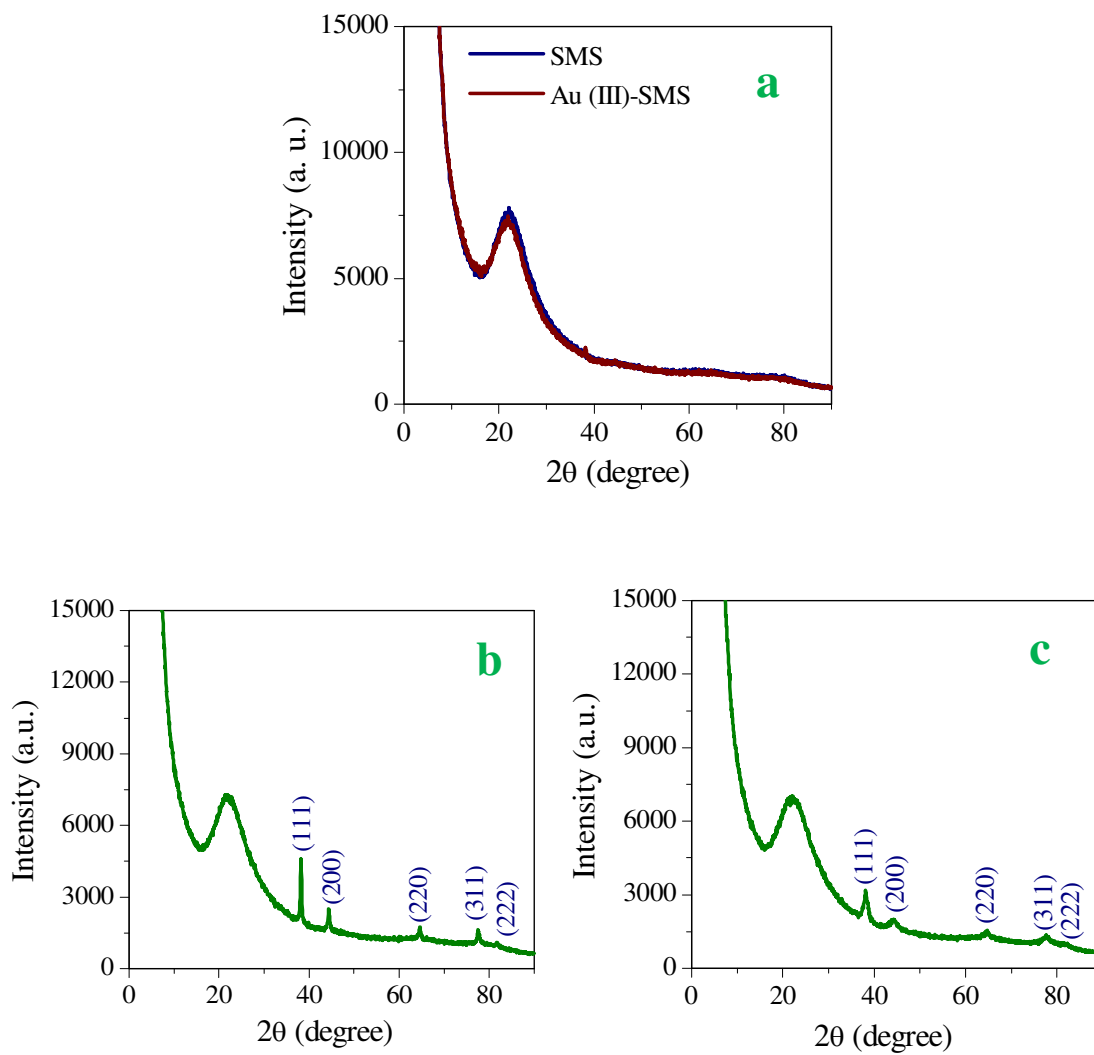


Fig. 1: XRD spectra of (a) SMS and Au(III)-SMS, (b) SMSG-1 (c) SMSG-2

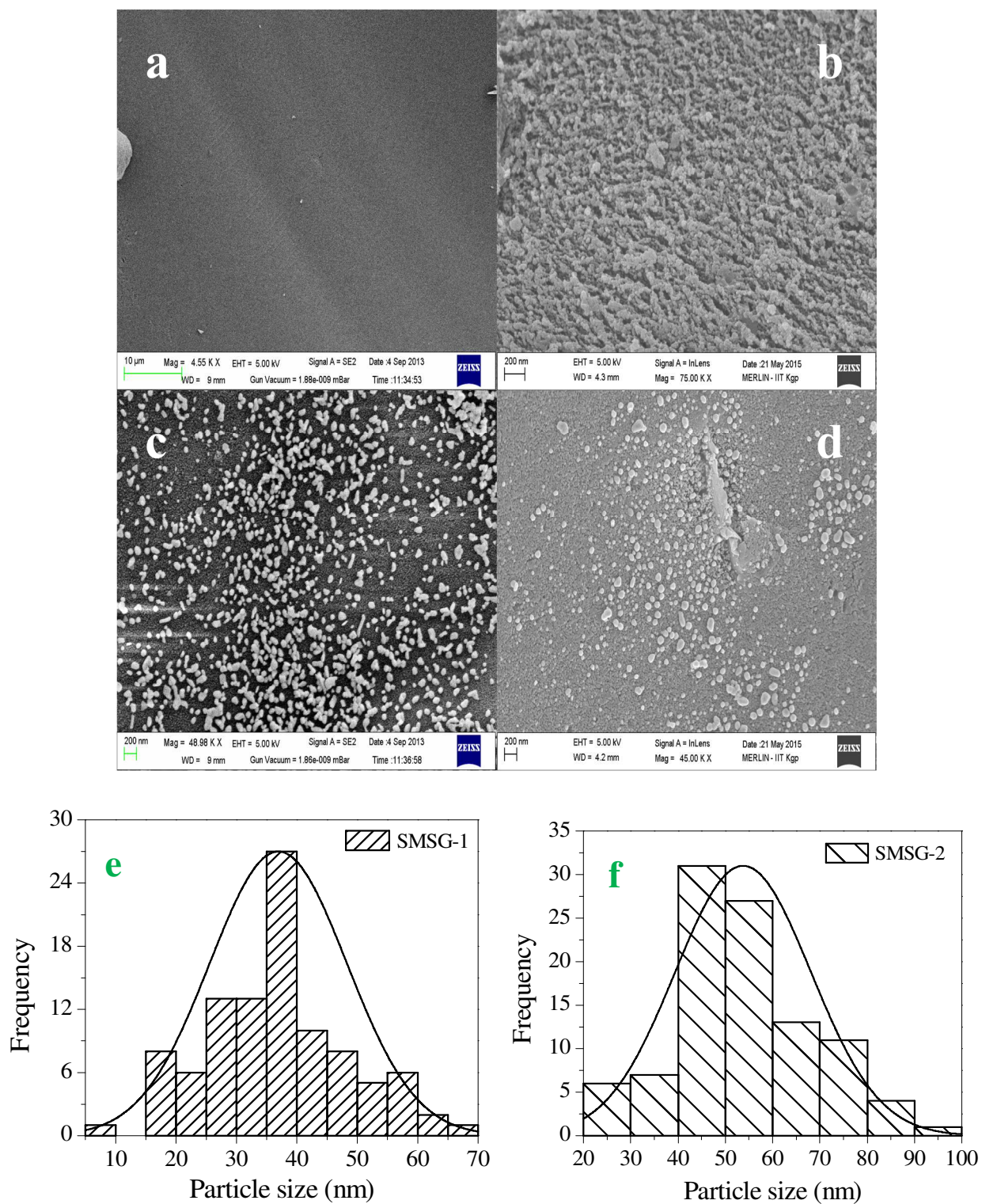


Fig. 2: SEM images of (a) SMS, (b) Au(III)-SMS, (c) SMSG-1, (d) SMSG-2. (e) and (f) shows the size distribution of Au(0) particles in SMSG-1 and SMSG-2, respectively.

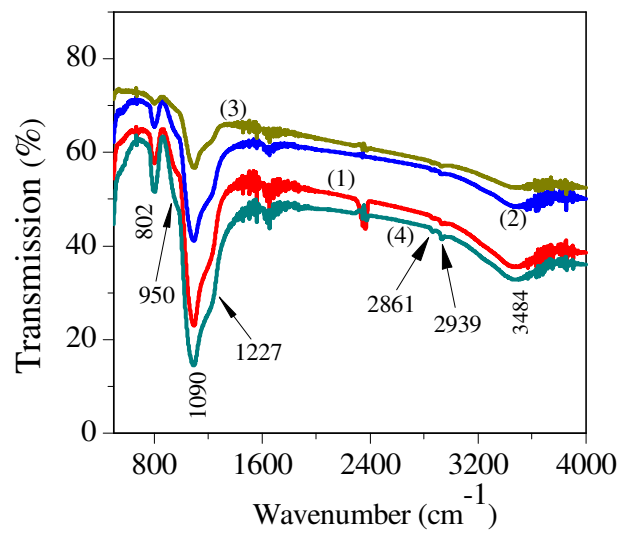


Fig. 3: FTIR spectra of (1) SMS, (2) Au(III)-SMS, (3) SMSG-1, (4) SMSG-2

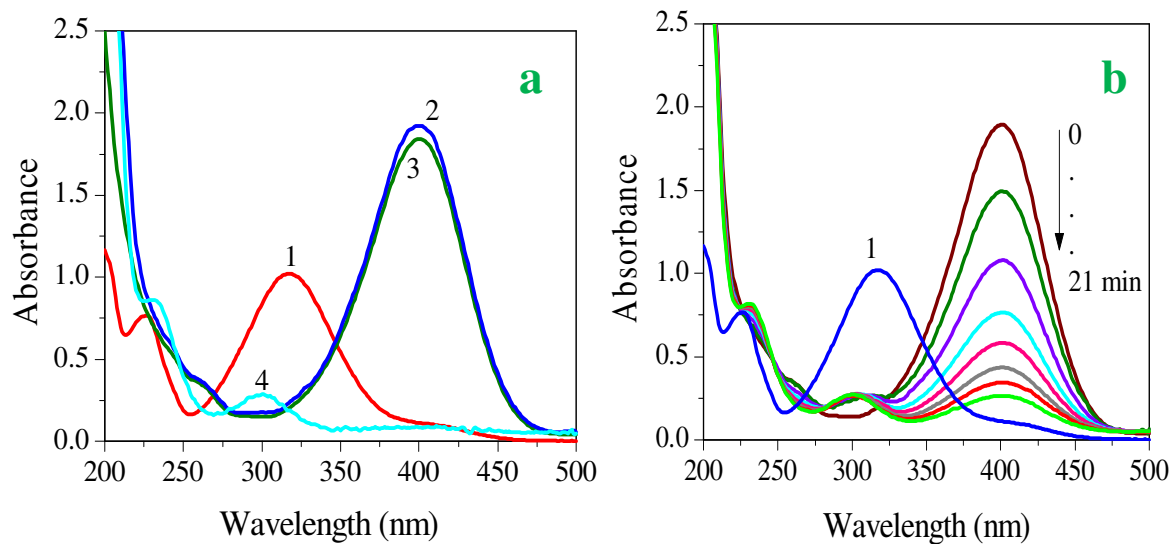


Fig. 4: (a) Absorption spectra of 4-NP under different conditions. Curve 1: 4-NP, curve 2: 4-NP+NaBH₄ (immediate), curve 3: 4-NP+SMS+NaBH₄ (after 20 min), curve 4: 4-NP+Au(III)-SMS+NaBH₄ (after 20 min) (Initial concentration of 4-NP = 1.0×10^{-4} M; Catalyst dose = 4 g/L). (b) Time dependent absorption spectra for the catalytic reduction of 4-NP in NaBH₄ medium by SMSG-1 as catalyst. Curve 1: 4-NP. (Initial concentration of 4-NP = 1.0×10^{-4} M; Catalyst dose = 3 g/L)

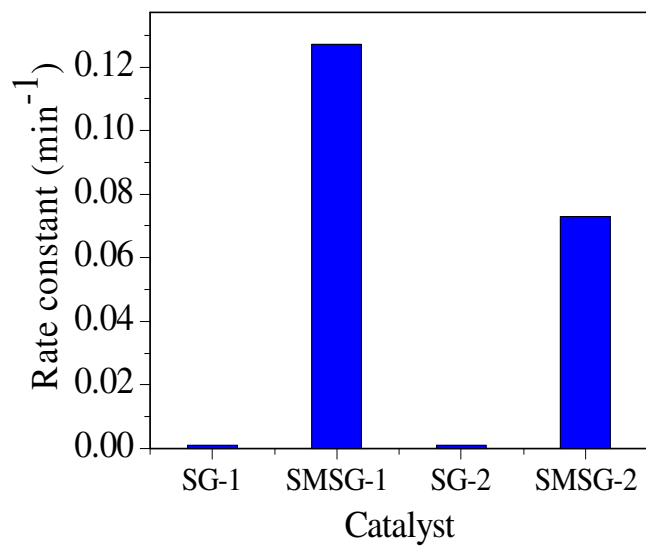


Fig. 5: A comparative account of pseudo-first order rate constant for 4-NP reduction using prepared catalysts SG-1, SMSG-1, SG-2 and SMSG-2 (Initial concentration of 4-NP = 1.0×10^{-4} M; Catalyst dose = 4 g/L)

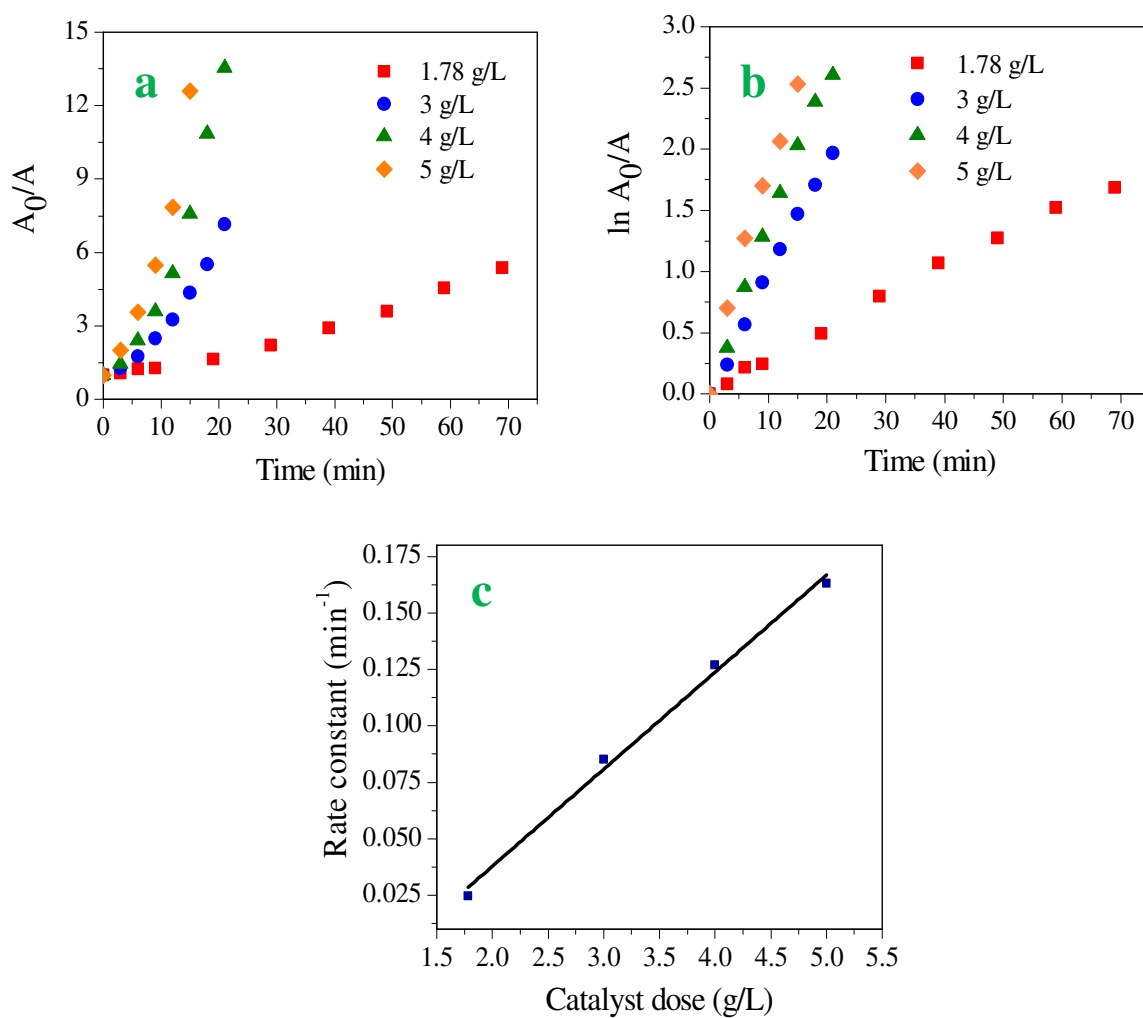


Fig. 6: Kinetics of 4-NP reduction in presence of SMSG-1 at different doses. (a) Plot of A_0/A vs. time. (b) Plot of $\ln A_0/A$ vs. time, (c) Plot of rate constant vs. catalyst dose (Initial concentration of 4-NP = 1.0×10^{-4} M, Concentration of NaBH_4 = 0.1 M)

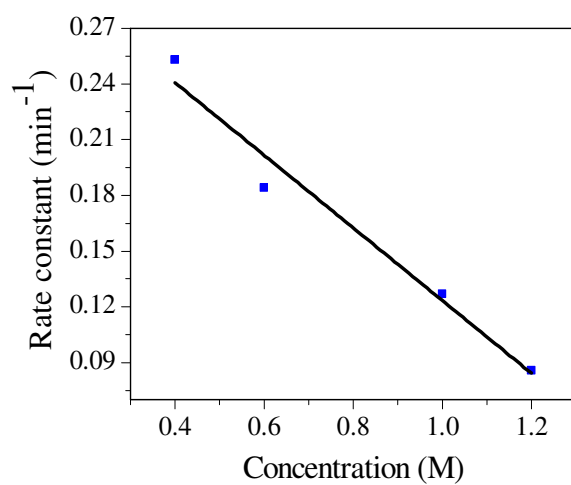


Fig. 7: Plot of rate constant vs. initial concentration of 4-NP for SMSG-1 (Catalyst dose = 4.0 g/L, Concentration of NaBH₄ = 0.1 M)

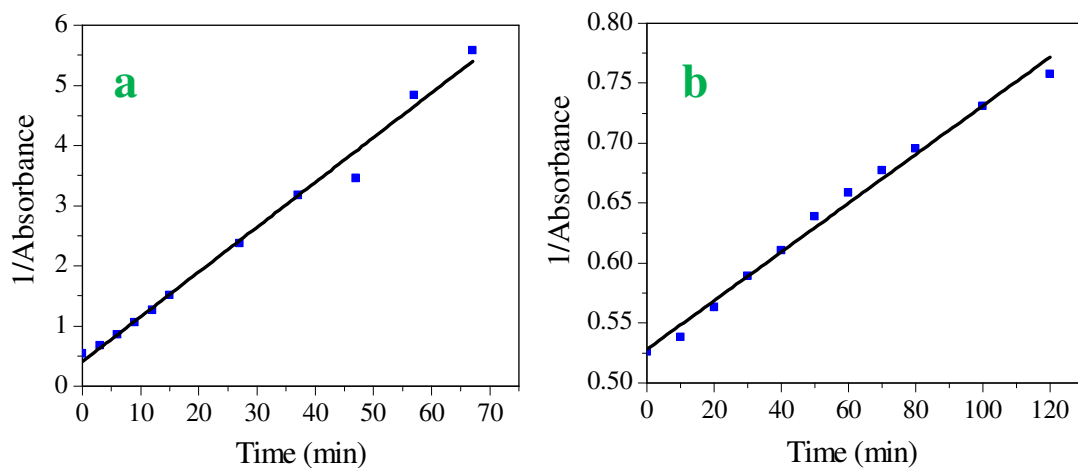


Fig. 8: (a) 1/Absorbance vs. time plot for 4-NP reduction with SMS-GME as catalyst, (b) 1/Absorbance vs. time plot with SMSG-2 (Initial concentration of 4-NP = 1.0×10^{-4} M, Dose of the catalyst = 0.2 g/L, Concentration of NaBH_4 = 0.1 M)

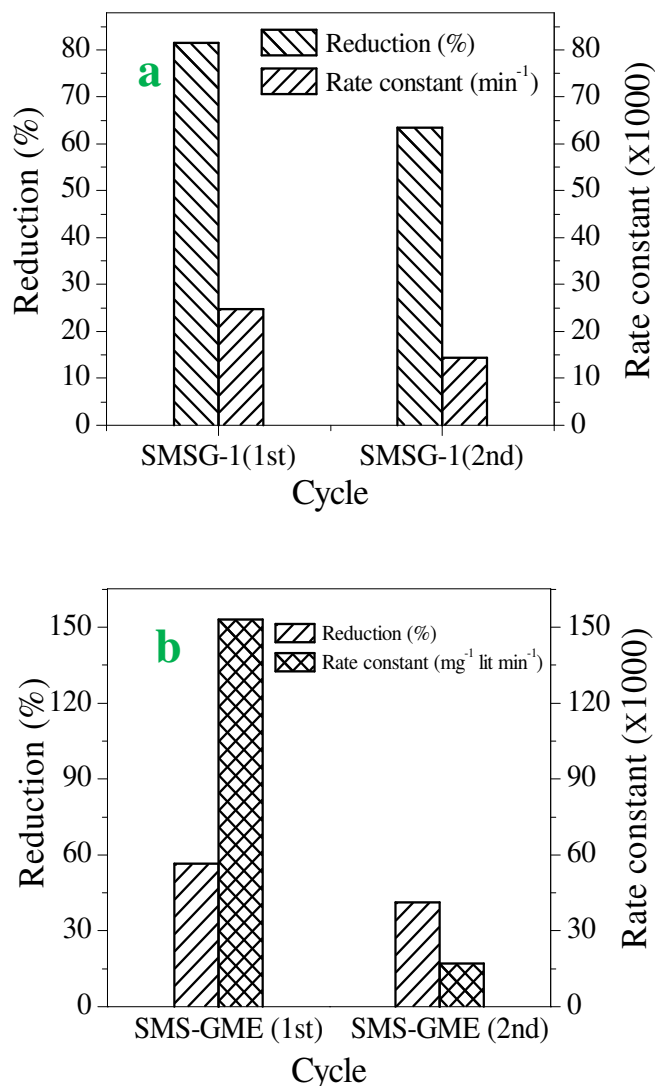


Fig. 9: (a) Plot of efficiency (after 70 min of reaction for both the cycles) and rate constant of 4-NP reduction in 1st and 2nd cycle using SMSG-1 (Initial concentration of 4-NP = 1.0×10^{-4} M, Catalyst dose = 1.78 g/L, Concentration of NaBH₄ = 0.1 M). (b) Plot of efficiency (after 10 min in case of 1st cycle and after 60 min in case of 2nd cycle) and rate constant of 4-NP reduction in 1st and 2nd cycle for SMS-GME (Initial concentration of 4-NP = 1.0×10^{-4} M, Catalyst dose = 0.5 g/L, Concentration of NaBH₄ = 0.1 M)

Table 1. Variation in rate constant of 4-NP reduction in presence of SMSG-1, SMSG-2 and SMSG-3 with respect to different kinetic parameters

Material	Dose of catalyst (g/L)	Initial conc. of 4-NP (M)	First order		Second order		Order of reaction followed
			Rate Constant min ⁻¹	R ²	Rate Constant mg ⁻¹ lit min ⁻¹	R ²	
SMSG-1	1.78	1.0×10 ⁻⁴	0.0248	0.996	0.034	0.974	first
	3	1.0×10 ⁻⁴	0.085	0.997	0.152	0.948	first
	4	1.0×10 ⁻⁴	0.127	0.993	0.289	0.931	first
	5	1.0×10 ⁻⁴	0.163	0.985	2.444	0.596	first
SMSG-1	4.0	0.4×10 ⁻⁴	0.253	0.967	1.186	0.966	first
	4.0	0.6×10 ⁻⁴	0.184	0.978	0.743	0.953	first
	4.0	1.0×10 ⁻⁴	0.127	0.993	0.289	0.931	first
	4.0	1.2×10 ⁻⁴	0.086	0.987	0.170	0.955	first
SMSG-2	1.78	1.0×10 ⁻⁴	0.014	0.968	0.013	0.996	second
	3	1.0×10 ⁻⁴	0.022	0.979	0.021	0.998	second
	3.5	1.0×10 ⁻⁴	0.026	0.961	0.038	0.998	second
	4	1.0×10 ⁻⁴	0.073	0.988	0.141	0.967	first
	5	1.0×10 ⁻⁴	0.085	0.995	0.130	0.967	first

SMSG-2	4.0	0.4×10^{-4}	0.033	0.954	0.075	0.983	second
	4.0	0.6×10^{-4}	0.028	0.961	0.071	0.987	second
	4.0	1.0×10^{-4}	0.073	0.988	0.141	0.967	first
	4.0	1.2×10^{-4}	0.059	0.990	0.131	0.962	first
SMS-GME	0.2	1.0×10^{-4}	0.076	0.960	0.031	0.998	second
SMSG-2	0.2	1.0×10^{-4}	0.002	0.979	0.003	0.990	second

Table 2. Comparison of pseudo-first order rate constants for the reduction of 4-NP using some selected Au (0) particles

Sl. No.	Catalyst	[4-NP] (M)	Dose of catalyst in terms of gold (g/L)	[NaBH ₄] (M)	Rate constant	Reference
1	Au-PMMA	4.3×10^{-4}	5.77×10^{-3}	0.63	$7.2-7.9 \times 10^{-3} \text{ s}^{-1}$	34
2	Au-Poly(AG- Co-VP)	6.7×10^{-4}	2.56×10^{-4}	0.067	$7.36 \times 10^{-3} \text{ s}^{-1}$	37
3	Au-ZnO powder	0.5×10^{-3}	3.28×10^{-2}	0.05	$7.6 \times 10^{-3} \text{ s}^{-1}$	17
4	Au/graphene	1.0×10^{-4}	0.753×10^{-3}	0.1	$3.17 \times 10^{-3} \text{ s}^{-1}$	39
5	Au@RMFNS ^a	2×10^{-4}	2.19×10^{-3}	0.0056	$33 \times 10^{-3} \text{ s}^{-1}$	40
6	SMSG-1	0.4×10^{-4}	5.0×10^{-2}	0.1	$4.22 \times 10^{-3} \text{ s}^{-1}$	This work

^a Resorcinol-melamine-formaldehyde resin nanospheres